 

https://doi.org/10.1070/QEL18043

# Generation and dynamics of wave packets with a large phase modulation depth

A.S. Abramov, I.O. Zolotovskii, D.A. Korobko, V.A. Kamynin, V.A. Ribenek, A.A. Fotiadi, V.S. Tsarev

***Abstract.*** **This paper examines the generation of high-frequency picosecond pulse trains as a result of modulation instability of wave packets with a large phase modulation depth and small amplitude modulation depth. We demonstrate that intermediate amplification of such wave packets and subsequent phase-to-amplitude modulation conversion lead to the formation of pulses with peak powers orders of magnitude higher than their initial power. The corresponding pulse generators can be used to generate a line spectrum.**

***Keywords:*** *modulation instability, phase modulation, amplitude modulation, ultrashort pulses, generation of a line spectrum.*

## 1. Introduction

Modulation instability (MI) is known to be a fundamental nonlinear process that leads to instability growth in physical systems [1, 2]. In optics, this effect shows up as the breaking of a modulated continuous wave into a pulse train [2, 3]. In addition, it is well known that MI can be 'used' for generation of a train of short optical pulses with a controllable repetition rate [4–10].

In this work, to obtain a train of picosecond pulses, we propose using MI of wave packets (WPs) with an initially strong phase modulation and weak amplitude modulation. For this purpose, we propose that a fibre ring cavity containing a narrow-band amplifier and phase modulator be used as a master oscillator ensuring the formation of required pulses. We demonstrate that, as a result of intermediate amplification of such WPs and subsequent conversion of phase modulation into amplitude modulation, the development of the induced MI regime leads to the formation of trains of ultrashort pulses (USPs). The peak power of the forming pulses is orders of magnitude higher than the optical power at the output of the ring master oscillator. At the same time, the repetition rate of the forming USPs turns out to be essentially equal to the frequency of the modulator present in the cavity. The proposed method shows significant similarity to so-called direct Fourier synthesis of pulses, considered by Eigenwillig et al. [11] and Lobach et al. [12].

**A.S. Abramov, I.O. Zolotovskii, D.A. Korobko, V.A. Ribenek, A.A. Fotiadi** Ulyanovsk State University, ul. L. Tolstogo 42, 432017 Ulyanovsk, Russia; e-mail: aleksei__abramov@mail.ru;
**V.A. Kamynin** Prokhorov General Physics Institute of the Russian Academy of Sciences, ul. Vavilova 38, 119991 Moscow, Russia;
**V.S. Tsarev** Ogarev Mordovia State University, Bol'shevistskaya ul. 68, 430005 Saransk, Mordovian Republic, Russia

Received 10 December 2021
*Kvantovaya Elektronika* **52** (5) 459–464 (2022)
Translated by O.M. Tsarev

## 2. Dynamics of quasi-cw light with a large phase modulation depth and a small amplitude modulation depth. Formation of giant pulses

We examine the dynamics of initially phase- and amplitude-modulated light propagating in longitudinally nonuniform fibre. Consider a WP for which initial conditions can be written in the form

$$A(z=0,t) \approx A_{\rm s}(t)\exp[{\rm i}\delta\cos(\Omega t)], \tag{1a}$$

where $A_{\rm s}(t)$ is a weakly modulated amplitude. At the input ($z=0$) of a waveguide modulator, it can be represented in the form

$$A_{\rm s}(z=0,t) \approx A_0[1+\delta_{\rm a}\cos(\Omega_{\rm a} t)]. \tag{1b}$$

In (1a) and (1b), the parameters $\delta$ and $\delta_{\rm a}$ determine the WP phase and amplitude modulation depths, respectively, at the waveguide modulator input, and $\Omega$ and $\Omega_{\rm a}$ determine the corresponding modulation frequencies. The signal is assumed to be initially weakly amplitude-modulated, i.e. $|\delta_{\rm a}| \ll 1$ and $|\delta_{\rm a}| \ll |\delta|$. In addition, the amplitude and phase modulation frequencies are taken to be almost identical $\Omega \approx \Omega_{\rm a}$.

In active fibre, the dynamics of a WP described by relations (1a) and (1b) is determined by the standard Schrödinger equation [1, 2, 8, 10]:

$$\frac{\partial A}{\partial z} - {\rm i}\frac{d_2}{2}\frac{\partial^2 A}{\partial \tau^2} - \frac{d_3}{6}\frac{\partial^3 A}{\partial \tau^3} + {\rm i}R\left(|A|^2 - \tau_{\rm R}\frac{\partial|A|^2}{\partial\tau}\right)A = gA, \tag{2}$$

where $R$ is the nonlinear parameter; the parameter $g$ characterises amplification (attenuation); $\tau_{\rm R}$ is the nonlinear response time; $\tau = t - z/u_{\rm gr}$ is retarded time; $u_{\rm gr}$ is the group velocity of the WP; and $d_2$ and $d_3$ are the second- and third-order dispersion parameters, respectively [1, 2, 10].

In the case of a WP with a large phase modulation depth, such that $|\alpha| = \delta\Omega^2/2 > 10^{24}\,{\rm s}^{-2}$, with allowance for the initial conditions (1a) and (1b) in the $d_3, \tau_{\rm R} \to 0$ approximation, the propagation equation (2) can be written in the form [13, 14]

$$\frac{\partial \bar{A}}{\partial z} - {\rm i}\frac{d_{2\rm eff}(z)}{2}\frac{\partial^2 \bar{A}}{\partial \tau'^2} + {\rm i}R_{\rm eff}(z)|\bar{A}|^2\bar{A} = -{\rm i}S(z)\tau'^2\bar{A}. \tag{3}$$

In (3), we introduce the parameters $\bar{A}(z,\tau) \approx A(z,\tau)\exp[-i\delta\cos(\Omega\tau) - Gz]$, $G = g - \alpha d_2$, $d_{2\text{eff}}(z) = d_2 f^2(z)$, $S(z) = 2\alpha^2 d_2 f^{-2}(z)$, and $R_{\text{eff}} = R\exp(2gz)$ and use the coordinates $z = z$ and $\tau' = f(z)\tau$, where $f(z) = \exp(-2\alpha d_2 z)$. Equation (3) is the Gross–Pitaevskii equation in which the effective dispersion parameter $d_{2\text{eff}}(z)$, effective nonlinear parameter $R_{\text{eff}}(z)$, and parabolic potential $S(z)$ are functions of the coordinate $z$.

WP instability in an external parabolic potential with no allowance for higher order dispersion effects has been the subject of several studies [13–17]. Prior to further examination, it is important to note that Eqn (3) has singular solutions at fibre lengths near $z_{\text{com}}$, which can be found numerically by solving the integral equation

$$\delta\Omega^2 d_2 z_{\text{com}} \approx 2. \tag{4}$$

MI in anomalous dispersion fibre ($d_2 < 0$ and $\delta < 0$) causes a wave packet of the form (1b) at $z \approx z_{\text{com}}$ to break up into pulses whose peak power far exceeds the background power [13, 14]. In this process, the repetition rate of the corresponding pulses remains essentially equal to the initial modulation frequency $\Omega$. Thus, as a result of MI and coherent summation of individual spectral components, a WP with a strong phase modulation and weak amplitude modulation should transform over a fibre length near $z_{\text{com}}$ into a train of USPs with a peak amplitude well above the average background power.

Note that, for superpulse generation over fibre lengths below 1 km at group velocity dispersion (GVD) $|d_2|$ of the order of $10^{-26}$ s$^2$ m$^{-1}$, the condition $|\delta|\Omega^2 > 10^{23}$ s$^{-2}$ should be fulfilled. At the same time, the modulation wavelength in 'standard' modulators meets the inequality $L_{\text{m}} \leqslant \pi c/(2n_0\Omega)$ [18, 19] (here, $n_0$ is the refractive index of the modulator). This imposes a limitation on the maximum possible phase modulation depth: $\delta_{\max} \propto \Delta n_{\max}\omega_0/\Omega < 10^{-4}\omega_0/\Omega$, where $\Delta n_{\max}$ is the maximum change in the refractive index in the corresponding waveguide modulator. Thus, in choosing standard refractive index modulation values, $\Delta n_{\max} = 10^{-4}$ to $10^{-6}$, we obtain a modulation depth considerably smaller than unity, $|\delta| < 1$, and as a consequence the superpulse formation condition is not met. In addition, we have the inequality $\alpha < \Delta n_{\max}\omega_0\Omega \ll 10^{23}$ s$^{-2}$.

The effective interaction length can be considerably increased in so-called travelling-wave modulators (TWMs) [18–21]. However, even with such modulators, modulation depths necessary for producing superpulses are difficult to achieve. In particular, in the case of TWMs with a modulation frequency in the range 1–10 GHz, characteristic refractive index modulation values are $\Delta n_{\max} \leqslant 1.5 \times 10^{-5}$ [18–20]. The condition that the modulation depth be small can then be written in the form $\delta \approx k_0\Delta n_{\max} l \approx 2\pi\Delta n_{\max} l/\lambda_0 < 1$, where $l$ is the modulator length.

If the input centre wavelength is $\lambda_0 \approx 1.55$ μm, this condition is fulfilled at a TWM length in the range $l \approx 1$–$2$ cm. On the other hand, in the corresponding range of modulation frequencies in typical TWMs, e.g. in those based on lithium niobate crystals, the travelling wavelength of a control electric field does not exceed 3 mm [19, 20], so the achievable modulation depth at such TWM lengths is $\delta \leqslant 0.15$. Note also that the presence of a TWM in a cavity markedly increases the cavity loss. Besides, such modulators cannot always ensure spatial beam parameters necessary for implementing the proposed configuration.

Classic TWMs are essentially incapable of ensuring the formation of WPs with ultrastrong modulation, $\delta \gg 10$, because the travelling wavelength of the control field should then exceed 1 m, which is inconsistent with the capabilities of the existing TWMs. At the same time, ultrastrong modulation can be of particular interest for WPs with a relatively low modulation frequency, $\Omega < 10^{10}$ s$^{-1}$. The use of WPs with such characteristics opens up the possibility of generating pulses with huge peak powers, far above 1 MW.

Thus, superpulse generation with the use of classic modulators, including TWMs, presents serious technical difficulties. At the same time, we do not rule out that high-frequency modulators ensuring large modulation depths will appear in the nearest future. Such modulators would substantially simplify implementation of the configuration in question.

Below, we present an alternative technique for the generation of WPs of the form (1) with a modulation depth and frequency $|\delta_{\text{eff}}| \approx 1$ and $\Omega > 10^{11}$ s$^{-1}$, respectively, with the use of a fibre ring cavity.

## 3. Ring configuration of lasing with a large phase modulation depth

In the simplest case, the proposed ring configuration (Fig. 1) comprises a phase modulator (*1*), narrow-band amplifier (*2*), broadband filter (*3*), and light outcoupling device. The parameters of all the components of the ring cavity are listed in Table 1.

The phase modulator, needed to obtain the required phase difference, is characterised by its transmission function $F = T_{\text{m}}\exp[i\delta\cos(\Omega\tau)]$, where $T_{\text{m}}$ is the single-pass amplitude loss in the modulator. The amplifier is used to maintain the required energy balance in the cavity – primarily, to compensate for the losses resulting from the subsequent filtering of the forming pulse train and the partial outcoupling of the light from the cavity in each pass. In our case, it is assumed that 1% of the light is outcoupled in each pass. Besides, we take into account the unavoidable loss in the phase modulator, which is 0.8 in our case. The gain coefficient of the amplifier can be represented in the form

$$g(\omega) = \frac{g_0}{1 + (\omega - \omega_{\text{r}})^2/\Delta\Omega^2}, \tag{5}$$

where $g_0$ is the gain at the resonance frequency; $\Omega_{\text{r}}$ is the resonance frequency of the gain line; and $\Delta\Omega$ is the gain linewidth.

**Table 1.** Parameters of the ring cavity.

| Modulator *1* | | Amplifier *2* | | | | | Filter *3* | |
|---|---|---|---|---|---|---|---|---|
| modulation depth $\delta$ | modulation frequency $\Omega$/s$^{-1}$ | gain $g_0$/m$^{-1}$ | gain linewidth $\Delta\Omega$/s$^{-1}$ | GVD $d_2$/s$^2$ m$^{-1}$ | nonlinearity $R$/W$^{-1}$ m$^{-1}$ | length/m | transmission $T_0$ | transmission bandwidt $\Delta\omega_{\text{lin}}$/s$^{-1}$ |
| –0.1 | $2 \times 10^{11}$ (33.3 GHz) | 0.38 | $10^6$ | $10^{-27}$ | $10^{-3}$ | 1 | 0.9 | $10^{12}$ |

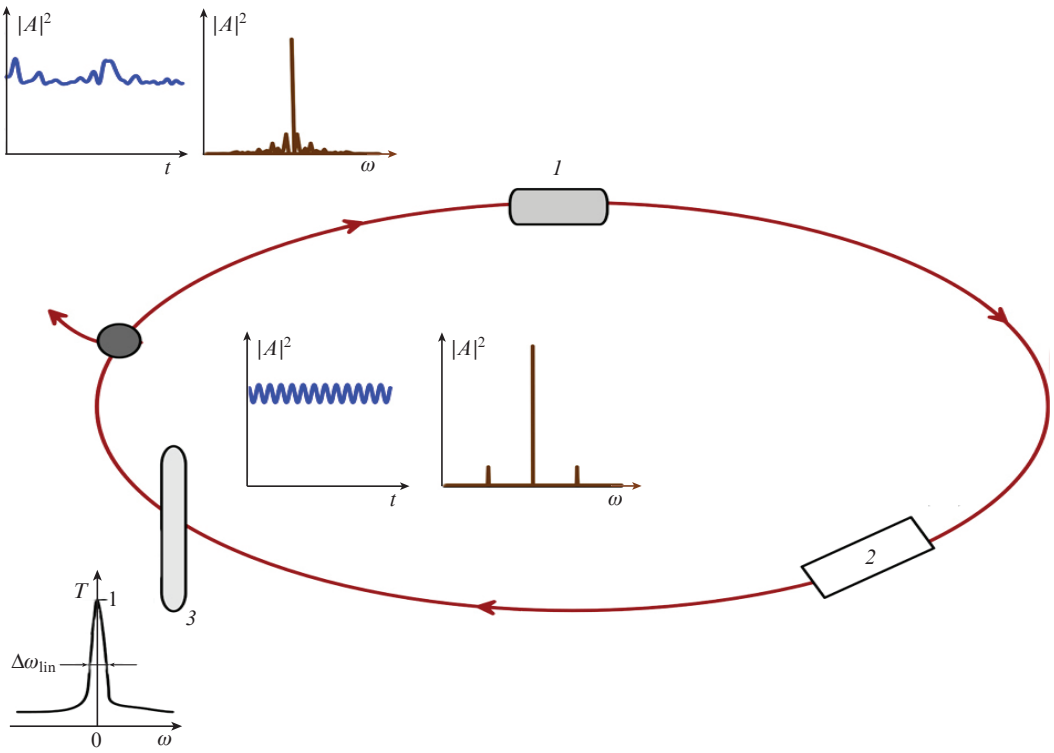


**Figure 1.** Ring cavity containing a phase modulator (see text for designations).

The amplifier in the proposed configuration has the form of active fibre with a small gain coefficient $g_0$ and a rather narrow gain line, e.g. a narrow-band Brillouin amplifier with a standard linewidth $\Delta\Omega$ in the range $10^6$ to $10^7$ s$^{-1}$. In effect, such an amplifier acts as a frequency filter, amplifying only in a narrow spectral region [21–23].

The last component of the ring cavity is a broadband filter with a bandwidth $\Delta\omega_{\rm lin}$. The filter is needed for a central spectral region, which will correspond to the main set of the brightest spectral lines in the output spectrum, to be separated from the overall frequency range. The transmission of the filter (Fig. 1) is given by

$$T = T_0 \exp\left[-\left(\frac{\omega - \omega_{\rm r}}{\Delta\omega_{\rm lin}}\right)^2\right]. \qquad (6)$$

Besides, we take transmission in the operating frequency range to be $T_0 \approx 0.9$, which characterises the optical loss in the corresponding filter.

The ring oscillator under consideration ensures the formation of WPs with a strong phase modulation and a relatively weak amplitude modulation. Such emission has a line spectrum (Fig. 2) dominated by the central line. At the cavity output, the WP amplitude will then be weakly modulated (upper inset), whereas the WP phase will be strongly modulated (lower inset), and both will be determined by the initial modulation depth and frequency, in accordance with relations (1). The frequency spacing between the generated lines will exactly coincide with the modulation frequency, $\Omega = 2 \times 10^{11}$ s$^{-1}$. The total width of the line spectrum, $\Delta\omega$, will be related to the modulation depth and frequency by $\Delta\omega \approx |\delta_{\rm eff}\Omega|$, where $|\delta_{\rm eff}| \approx |(\varphi_{\max} - \varphi_{\min})/2|$.

The use of the ring oscillator makes it possible to substantially increase the phase modulation depth. In our case, the phase difference increases by about one order of magnitude (Fig. 2, lower inset). Note that, in the 'linear' configuration under consideration, the phase modulation depth increases and the amplitude modulation depth decreases with decreasing

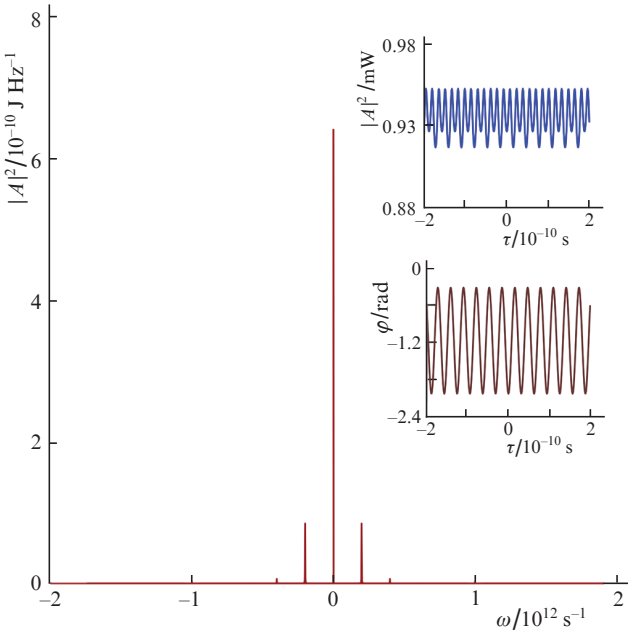


**Figure 2.** Emission spectrum of a ring cavity laser in stable lasing mode. Insets: WP amplitude and phase $\varphi$.

amplifier bandwidth. This suggests that it is the Brillouin amplifiers [21–23] mentioned above which can be the most effective in implementing the appropriate lasing configuration.

It is seen from Fig. 2 that, in the case under consideration, we have $\delta_{\text{eff}} \approx -1$, i.e. the magnitude of the corresponding modulation depth is about one order of magnitude larger than the depth that can be ensured by the modulator used in the ring configuration. At the same time, the amplitude modulation depth $\delta_a$ remains essentially unchanged: $\sim 0.03 \times 10^{-3}$. As a consequence, the amplitude of the central line remains considerably larger than those of the other lines, and this results in cw (weakly amplitude-modulated) lasing mode of the proposed ring oscillator.

Thus, at the ring cavity output we obtain quasi-cw light with weak amplitude modulation and strong phase modulation (Fig. 2, insets). As a consequence, the initial emission spectrum transforms into a set of spectral lines, where the main (central) line has the highest intensity and, farther away from it, the peak intensity of the side lines decreases appreciably. The spacing between two neighbouring spectral lines is equal to the modulation frequency.

Note that, unlike in the case of classic mode locking, which requires that the cavity round-trip time be matched to the modulation frequency, this is not necessary in the case under consideration. The field in the ring cavity is quasi-uniform in intensity, weakly modulated in time and along the coordinate. Therefore, the configuration in question differs significantly from the 'classic' active mode locking scheme [1, 18, 24–26].

## 4. Cascaded fibre configuration for generation of USPs with a broad line spectrum

To generate trains of USPs having a broad line spectrum, the ring cavity configuration considered above should be supplemented with a fibre cascade comprising passive and active fibres. Figure 3 shows a schematic of a USP generator, and Table 2 presents calculated parameters of the additional fibres (cascade elements *4–6*). The nonlinear response time $\tau_R$ and GVD $d_3$ were taken to be identical for all cascade elements: $\tau_R \approx 3$ fs and $d_3 = 10^{-41}$ s$^3$ m$^{-1}$.

The dynamics of light in the cascade can in this case be described by the nonlinear Schrödinger equation (2), and the output parameters of the fibre generator considered above are used as initial conditions for the light launched into the fibre cascade. The strongly phase-modulated light generated by it (master oscillator) is launched into the fibre cascade (*4–6*), where a stable pulse train is formed over a length roughly equal to $z_{\text{com}}$ owing to intermediate amplification and phase-to-amplitude modulation conversion,

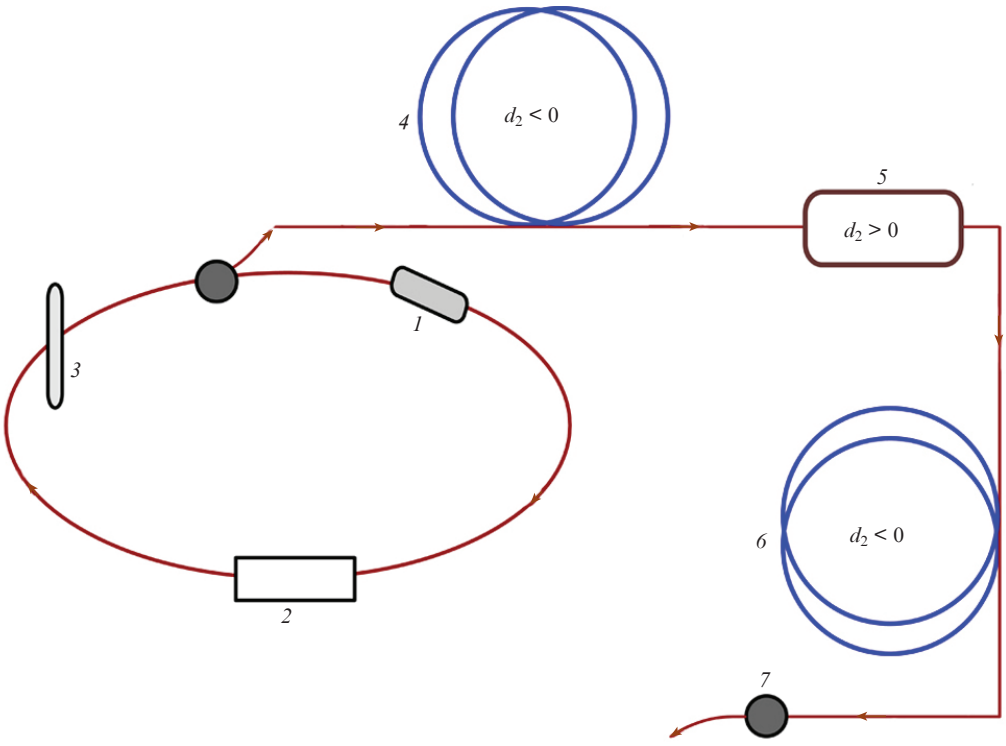


**Figure 3.** Schematic illustrating the formation (generation) of high-repetition-rate USP trains: (1) modulator; (2) narrow-band fibre amplifier; (3) filter; (4, 6) passive fibres; (5) broadband fibre amplifier; (7) output coupler.

**Table 2.** Calculated parameters of the cascade comprising passive (*4*, *6*) and active (*5*) fibres.

| Passive fibres *4*, *6* | | | Active fibre *5* | | | | |
|---|---|---|---|---|---|---|---|
| GVD $d_2$/s$^2$ m$^{-1}$ | nonlinearity $R$/W$^{-1}$ m$^{-1}$ | length/m | GVD $d_2$/s$^2$ m$^{-1}$ | nonlinearity $R$/W$^{-1}$ m$^{-1}$ | length/m | gain $g_0$/m$^{-1}$ | gain linewidth $\Delta\omega_{\text{lin}}$/s$^{-1}$ |
| $-5 \times 10^{-26}$ | 0.005 | 800 (*4*)<br>480, 200, 180 (*6*) | $10^{-26}$ | 0.005 | 1 | 3.9 | $10^{11}$, $4 \times 10^{11}$, $10^{12}$ |

which is accompanied by a sharp increase in pulse peak power. The amplifying fibre (*5*) in the cascade is needed for raising the average power of the modulated light and, hence, the peak power of the pulses resulting from further MI development.

At the parameters chosen, stable and sufficiently perfect picosecond pulse trains will be observed at the output of the system. Figure 4a shows generated USP trains after the cascade of passive and active fibres at gain linewidths $\Delta\omega_{lin} = 10^{11}$, $4 \times 10^{11}$ and $10^{12}$ s$^{-1}$. At the parameters chosen, the pulse repetition rate is determined with high accuracy by the modulation frequency of the phase modulator in the ring oscillator, $\Omega$, and the pulse peak power depends on the gain coefficients and linewidths of amplifiers *2* and *5*. According to our calculations, it is optimal to use amplifiers with the maximum possible gain linewidth in the fibre cascade (Fig. 4a), because they are capable of ensuring the highest USP peak power. Besides, at a larger amplifier linewidth, the superpulse formation length is determined by relation (4) with higher accuracy.

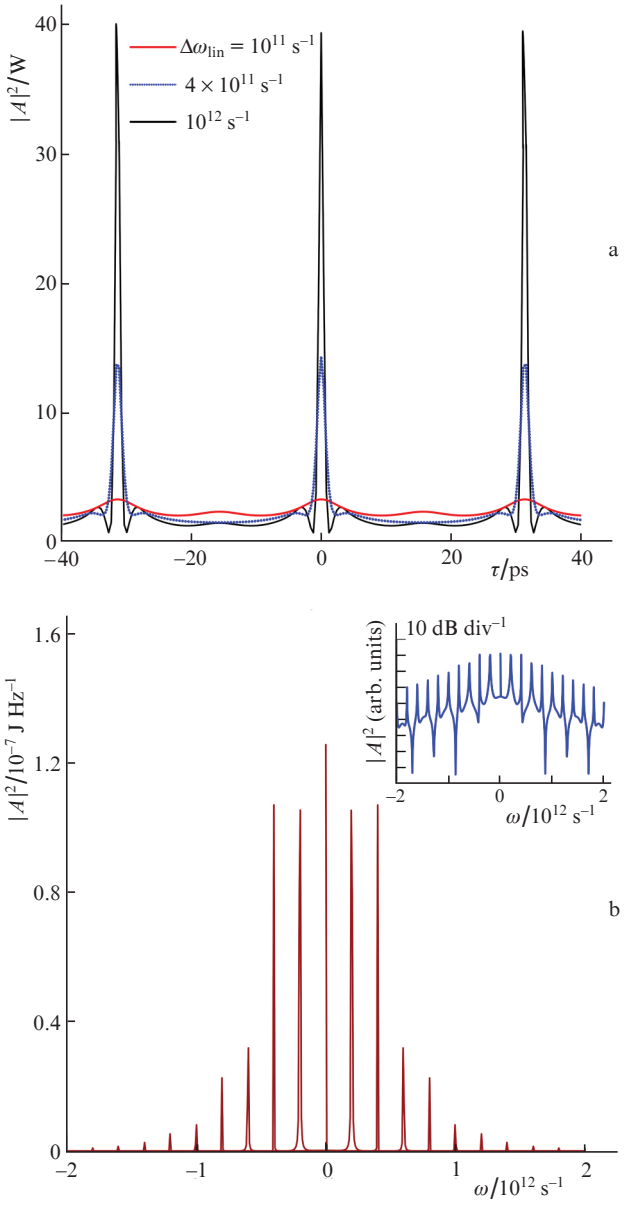


**Figure 4.** (a) Pulse power as a function of gain linewidth $\Delta\omega_{lin}$ and (b) emission spectrum at $\Delta\omega_{lin} = 10^{12}$ s$^{-1}$ after the ring cavity and the cascade of passive and active fibres. Inset: spectrum on a semilog plot. The parameters of the fibres are given in Table 2.

Of special note is that the spectral width of generated pulses exceeds the luminescence linewidth of the active fibre. Thus, it is desirable to use a narrow-band amplifier in the ring oscillator configuration under consideration and an amplifier with the widest possible gain band in the cascaded gain element.

It seems likely that an optimal gain element of the master oscillator is a narrow-band Brillouin amplifier, whereas that of the cascade is a Raman or parametric amplifier with the widest possible gain band. Of special importance is that USPs at their formation point will also have a line spectrum (Fig. 4b). As a consequence, the described system can be regarded as a fibre generator of a line spectrum, a so-called comb generator [27–29], with a spectral brightness of individual components exceeding the average level.

The final width of individual lines in the forming line spectrum is determined by several factors. The most important role is played by nonlinear effects, primarily, by MI due to four-wave interaction. In the general case, the question of the smallest possible width of individual spectral lines requires detailed analysis. It is reasonable to assert that, in the system considered here, with the fibre and input light parameters chosen, the comb linewidth is of the same order as the linewidth of the line spectrum generated by the master oscillator. This linewidth is in turn roughly equal to the gain linewidth of the active medium of the master oscillator.

That the even and odd harmonics of the line spectrum in Fig. 4b differ in shape and width can be accounted for as follows: The output of the master oscillator is a train of long chirped pulses whose repetition rate is equal to the modulation frequency. At the same time, the oscillation period of WPs (equal to the modulation period) turns out to be considerably shorter than their duration. The WP duration is roughly equal to the inverse of the gain linewidth of the active medium of the master oscillator. The shape of the corresponding pulses (Fig. 2, upper inset) is such that there is a small local 'dip' in their central part, corresponding to the region of the minimum in the phase of the WP. The amplitude and phase modulation asymmetry arising during generation (Fig. 2, insets) and the subsequent influence of nonlinear effects and further modulation instability development result in the spectrum shown in Fig. 4b.

## 5. Conclusions

A technique has been proposed for obtaining light with strong phase modulation and weak amplitude modulation using a ring cavity as a master oscillator. We have examined the formation of picosecond pulses with a subterahertz repetition rate from such initially cw light with a weak amplitude modulation. It is shown that the peak power of such pulses can be orders of magnitude higher than the power of the input quasi-cw light. We have examined the feasibility of using corresponding fibre cascades as all-fibre generators of a line spectrum. The use of broadband amplifiers with a gain linewidth above 10 nm opens up the possibility of generating pulses with huge peak powers (above 100 kW). The feasibility of generating such pulses will be discussed in our subsequent reports.

***Acknowledgements.*** This work was supported by the RF Ministry of Science and Higher Education [Megagrant Programme (Application No. 2020-220-08-1369) and RF President's Scholarship (Project No. SP-4058.2021.5)], the Russian Science Foundation (Grant No. 19-72-10037), and the Russian Foundation for Basic Research (Grant No. 19-42-730005).

## References

1. Agrawal G.P. *Nonlinear Fiber Optics* (Oxford: Academic Press, 2013).
2. Kivshar Yu.S., Agrawal G.P. *Optical Solitons: From Fibers to Photonic Crystals* (Academic Press, 2003).
3. Abdullaev F.Kh., Darmanyan S.A., Garnier J. *Prog. Opt.*, **44**, 303 (2002).
4. Mamyshev P.V., Chernikov S.V., Dianov E.M., Prokhorov A.M. *Opt. Lett*., **15**, 1365 (1990).
5. Chernikov S.V., Dianov E.M., Richardson D.J., Laming R.I., Payne D.N. *Appl. Phys. Lett*., **63**, 293 (1993).
6. Swanson E.A., Chinn S.R. *IEEE Photonics Technol. Lett*., **6**, 796 (1994).
7. Xu W., Zhang S., Chen W., Luo A., Liu S. *Opt. Commun.*, **199**, 355 (2001).
8. Erkintalo M., Hammani K., Kibler B., Finot C., Akhmediev N., Dudley J.N., Genty G. *Phys. Rev. Lett*., **107**, 253901 (2011).
9. Korobko D.A., Stoliarov D.A., Itrin P.A., Odnoblyudov M.A., Petrov A.B., Gumenyuk R.V. *Opt. Laser Technol*., **133**, 106526 (2021).
10. Panyaev I.S., Stoliarov D.A., Sysoliatin A.A., Zolotovskii I.O., Korobko D.A. *Quantum Electron*., **51**, 427 (2021) [*Kvantovaya Elektron*., **51**, 427 (2021)].
11. Eigenwillig C., Wieser W., Todor S., Biedermann B., Klein T., Jirauschek C., Huber R. *Nat. Commun*., **4**, 1848 (2013).
12. Lobach A., Kablukov S.I., Podivilov E.V., Fotiadi A.A., Babin S.A. *Opt. Lett*., **40**, 3671 (2015).
13. Zolotovskii I.O., Korobko D.A., Lapin V.A., Mironov P.P., Sementsov D.I., Yavtushenko M.S., Fotiadi A.A. *J. Opt. Soc. Am. B*, **36**, 2877 (2019).
14. Zolotovskii I.O., Korobko D.A., Lapin V.A., Mironov P.P., Sementsov D.I., Fotiadi A.A., Yavtushenko M.S. *Quantum Electron*., **48**, 818 (2018) [*Kvantovaya Elektron*., **48**, 818 (2018)].
15. Pitaevskii L.P. *Phys. Usp*., **49**, 333 (2006) [*Usp. Fiz. Nauk*, **176**, 345 (2006)].
16. Malomed B.A. *Soliton Management in Periodic Systems* (New York: Springer Science & Business Media, 2006).
17. Miroshnichenko A.E. *Rev. Mod. Phys*., **82**, 2257 (2010).
18. Yariv A., Yeh P. *Photonics: Optical Electronics in Modern Communications* (New York, Oxford: Oxford University Press, 2007).
19. Petrov V.M., Agruzov P.M., Lebedev V.V., Il'ichev I.V., Shamrai A.V. *Phys. Usp*., **64**, 722 (2021) [*Usp. Fiz. Nauk*, **191**, 760 (2021)].
20. Noguchi K., Mitomi O., Miyazawa H. *J. Lightwave Technol*., **16**, 615 (1998).
21. Kobyakov A., Sauer M., Chowdhury D. *Adv. Opt. Photonics*, **2**, 1 (2010).
22. Smith S.P., Zarinetchi F., Ezekiel S. *Opt. Lett*., **16**, 393 (1991).
23. Spirin V.V., López-Mercado C.A., Mégret P., Fotiadi A.A. *Laser Phys. Lett*., **9**, 377 (2012).
24. Siegman A.E., Kuizenga D.J. *Opt. Quantum Electron*., **6**, 43 (1974).
25. Kuizenga D.J., Siegman A.E. *IEEE J. Quantum Electron*., **QE-6**, 694; 709 (1970).
26. Kuizenga D.J., Phillion D.W., Lund T., Seigman A.S. *Opt. Commun*., **9**, 221 (1973).
27. Bandelow U., Radziunas M., Vladimirov A., Hüttl B., Kaiser R. *Opt. Quantum Electron*., **38**, 495 (2006).
28. Kippenberg T.J., Holzwarth R., Diddams S.A. *Science*, **332**, 6029 (2011).
29. Volkov I.A., Kamynin V.A., Itrin P.A., Ushakov S.N., Nishchev K.N., Tsvetkov V.B. *Quantum Electron*., **50**, 153 (2020) [*Kvantovaya Elektron*., **50**, 153 (2020)].